1 Introduction

Aerosols and water vapor are extremely important for the weather forecast and climate studies to predict dangerous situations. Aerosols are suspended particles for example sea-salts, mineral dust, organic matter and smoke. They enter the atmosphere from a variety of natural and anthropological sources and play an important role in countering global warming effects by reflecting incoming solar radiation and by influencing the hydro-logical cycle. Hence, aerosols play an important role in the complex climate system of the earth [1–3]. Water vapor is one of the most important atmosphere constitutes. It governs the atmosphere water cycle, which is the basic for life on earth and plays a crucial role in both radiation and convective energy transfer through the atmosphere [4–7]. Water vapor is a key gas with extreme and rapid variability, which is related to various atmosphere effects. Water is transported into the atmosphere via evaporation where the rate depends on the ocean and air temperature [8].

Accurate measurement of aerosols and water vapor in the atmosphere is necessary to understand its behavior. It is a key information for both the weather forecast and climate research. The main challenge of aerosols and water vapor detection is the variability of its prevalence [1–7]. It is essential to understand their spatial and temporal variability in relation to various atmospheric effects.

The concept of Light Detection and Ranging ($LIDAR$) systems was first introduced in the early 1960s after the invention of the laser [9]. The $LIDAR$ systems allow measuring the distribution of specific trace gas species in the atmosphere with a good accuracy and a sufficient spatial resolution [10, 11]. $LIDAR$ is a powerful tool for enhancing the knowledge and understanding of a wide variety of environmental phenomena which relate to the atmosphere, oceans, land surface, ice cover and finally to life [11]. It uses light in form of a pulsed laser which is transmitted through the atmosphere. Where it hits an object and scatters. A portion is scattered back to a detector system. Based on the arrival time of the backscattered, a spatial resolved distribution of particles, aerosols and molecules can be determined [12–14].

Differential absorption $LIDAR$ ($DIAL$) is a developed technique that operates at two wavelengths, one on resonance and one off resonance of the water vapor absorption line. The on resonance wavelength is more strongly absorbed than the off resonance wavelength. The difference between both back scattering signals is proportional to concentration of the water vapor [15–25]. Thus, the quantity of water vapor at a particular pinpointed location can be inferred.

Conventional $LIDAR$ systems use very high power (MW-peak power), ns pulse length, mJ peak energy at low repetition rates in the Hz-range. Solid state lasers such as Ti:Sapphire lasers [13, 14], Alexandrite lasers [15], optical parametric oscillators (OPO) [16], $Cr : LiSAF$ lasers [17, 18], and $Nd : YAG$ lasers [19, 20] were used. These lasers provide high pulse energies to achieve the necessary spatial and temporal resolution. Although yielding high pulse energy, the practical use of solid state lasers is not widely implemented in $LIDAR$ systems that require deployment in standalone network configurations. Due to the high maintenance cost, the replacement of pump sources and gain medium, the low electro-optical and optical-optical efficiencies, the large optical footprints and large nominal ocular hazard distances are detrimental [26].

An alternative approach known as the Micro Pulse $Lidar$ (MPL) system was used [27–29]. The first MPL was developed by $NASA's$ Goddard Space Flight Centre in 1993. In MPL systems, the repetition rates (f) are increased to approximately some 10 kHz and the pulse length (τ) shortened to a few μs. The large signal-to-noise ratio can be achieved by summing over millions of pulses in fairly short time intervals of several minutes. This allows to reduce the pulse energies to the μJ ranges. The low pulse energy is an important factor for eye-safety systems. A diode pumped $Nd : YAG$ laser was used because of the availability and their suited properties.

Recent progress in diode laser technology allowed an improvement of the vertical layer structures by the introduction of super large optical cavities and herewith reduction of the facet load. The development of a highly reliable mirror technology by applying cleaning and passivation techniques and the use of highly reliable mirror coating are demonstrated. An all diode laser system becomes feasible to reach a peak power above 10 W [27, 30–33]. Master oscillator power amplifier ($MOPA$) systems in which a distributed Bragg reflector (DBR) laser, a distributed feedback (DFB) laser, or an external cavity diode laser ($ECDL$) acts as master oscillator (MO) and a tapered amplifier acts as power amplifier (PA). The MO offers a stabilized wavelength and a small spectral line width whereas the PA provides a high output power.

The $MOPA$ systems have the capability to reach a peak power in the range of 10 W and the output energy in the μJ range. A $MOPA$ is powerful enough to be used as an all semiconductor laser transmitter in $LIDAR$ or $DIAL$ for aerosols and water vapor detection. They are not only compact, inexpensive, highly efficient, mechanically stable, but also feature widely varied wavelengths. This allows to select a precise wavelength at absorption lines for each molecular atmospheric composition to achieve an optimal efficient detection. This thesis demonstrates all-diode lasers based $MOPA$ systems. The developed systems show the potentially applicable in $LIDAR$ or $DIAL$ systems for aerosols and water vapor detection and allow ultra-compact, low cost systems and can be known as Micro Pulse Lidar systems ($MPLs$).

This work is organized as follows:

- The second chapter discusses the principles of operating $LIDAR$ systems as well as gaining understanding of the requirements of the laser transmitters for $LIDAR$ systems. Then the specifications of the light source for elastic-backscatter $LIDAR$ system for aerosols are derived. For more accuracy and higher resolution, e.g, water vapor profiling, the differential absorption $LIDAR$ ($DIAL$) is introduced. Success in $MPLs$ development is strongly connected with particular laser technology. A certain $MPLs$ technique needs specifically designed laser transmissions. For this reason, specific parameters of the laser systems in this work will be discussed. Then the status of the diode laser based $MOPA$ systems as laser transmitters for aerosols and water vapor will be shown.

- The third chapter will present the approaches of the $MOPA$ concepts. A short description of the fabrication of the monolithic $MOPA$ and the individual devices of hybrid $MOPA$ systems used in this work will be given.

- For characterization of diode lasers and $MOPA$ systems, the experimental setups are comprised in chapter four. Basic characterization such as electro-optical characterization, spectral properties under continuous wave mode and under the ns-pulse excitation are shown. A description of the electrical circuit for high currents and short pulses will be discussed.

- Chapter five goes into details of the experimental results of the wavelength stabilized diode laser based $ns-MOPA$ systems. Two concepts of monolithic and hybrid $MOPA$ systems operation at 1064 nm are investigated. One is a monolithic $MOPA$ and another is a hybrid $MOPA$ system. The monolithic $MOPA$ is a compact approach with integrated MO and PA on a single chip. The hybrid $MOPA$ system consists of a DFB laser and a multi-section amplifier. Based on specification of two concepts further investigation is oriented. The hybrid $MOPA$ system is suitable for atmospheric gases as well as for aerosols measurement whereas the monolithic $MOPA$ is sufficient only for aerosols.

- For concentration calibration, adjustment of the working points and the selection of suitable absorption lines, the laser transmitters need not only to be stable at a specific wavelength but also must be tuned continuously to scan over more than one absorption line. Chapter six presents a tunable wavelength hybrid $MOPA$ system. It operates at wavelengths of around 975 nm where one potential spectral region for water vapor detection is located. The behavior of the output power on the input power as well as saturated operation of the system will be discussed. The delay time between the optical gate and tapered section targeting of a small of amount of amplified spontaneous emission is investigated. Then the spectral tuning range of 0.9 nm will be shown. It is possible to scan over several absorption lines of water vapor.

- Chapter seven describes an investigation of a $MOPA$ system operation at two wavelengths for an application in differential absorption $LIDAR$ ($DIAL$) systems. The $MOPA$ uses a dual wavelength $Y-branch-DFB$ laser and a multi-section tapered amplifier.

It features two wavelengths at around of 964 nm. By changing the temperatures and currents of the $Y - branch - DFB$ the tuning of two wavelengths is achieved. Two pair wavelengths for on-off lines with different absorption coefficients of water vapor are selected. The peak power, spectral line widths and $SMSR$ at each wavelength are given.

- Finally, summary and outlines of future areas of interest for the extension of the ideas developed in this work will be shown in chapter eight.

2 Basic principle of LIDAR and DIAL systems-light sources for LIDAR and DIAL

2.1 Basic principle of LIDAR system and basic equation

In order to understand the needs of the $MOPA$ light sources in the $LIDAR$ or $DIAL$ systems, a short overview of the operation principle of the $LIDAR$ system is given in this part. The $LIDAR$ equation is introduced to analyze the contribution of each parameter of the laser transmitter in such a system.

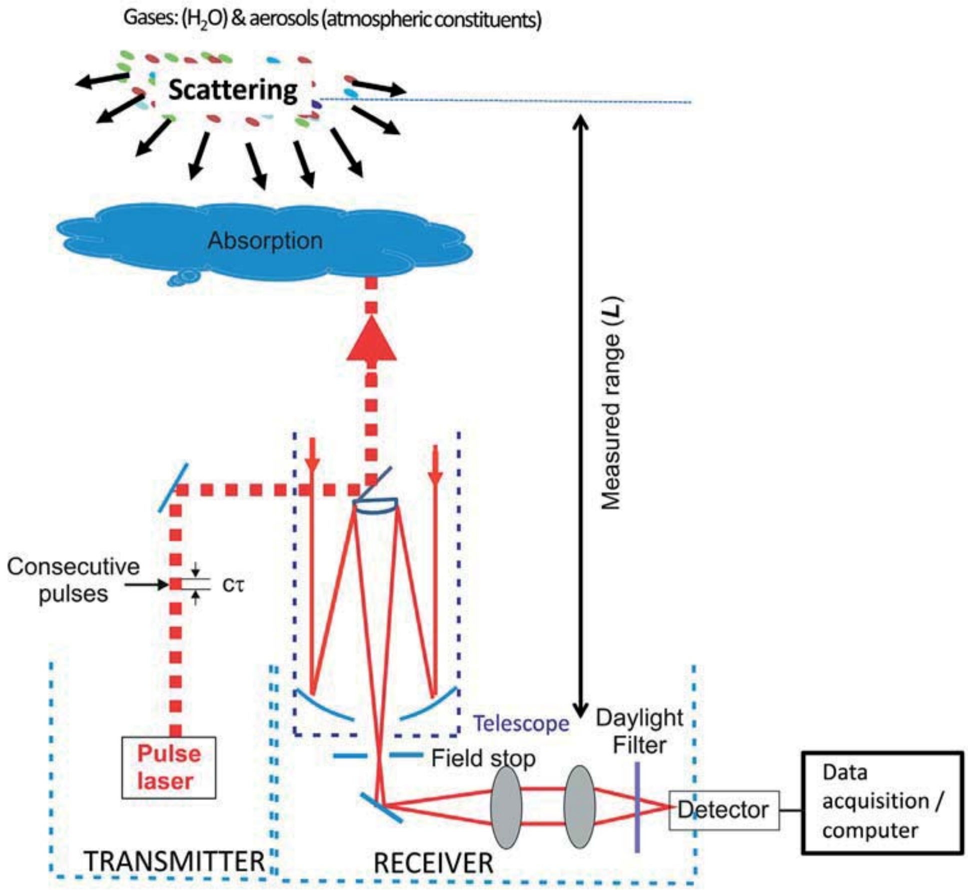

Figure 2.1: Schematic diagram of LIDAR system block diagram.

A principle scheme of the $LIDAR$ is given in Fig 2.1. In the simplest term, it consists of a transmitter and a receiver. Short laser pulses with lengths of few to several hundreds of nanoseconds and specific spectral properties are generated by a laser. The collimated light beam is sent into the atmosphere. It can be absorbed and scattered by atmospheric constituents. At the receiver, a telescope collects the photons backscattered from the atmosphere then passes through a field stop placed at the focus plane of the telescope. The field stop limits the field of view such that returns from multiple scattering events and stray background light are prevented before reaching the detector. A narrow optical filter placed in front of the detector is to ensure that only the backscattered light from the laser transmitter is measured by the detector. The duration time of each scattering event from a single laser pulse is proportional to the distance to the scattering volume along the entire illuminated path. The signal processing and data acquisition are analyzed to inform the characterization of the extent and properties of aerosols, gases such as water vapor or other particles based on the real-time detection and post-processing of the signal return.

The received power $P(\lambda, R)$ from a distance R at a wavelength λ can be calculated by the $LIDAR$ equation, written in ref.[34] for a single scatter, monochromatic elastic $LIDAR$ with the simplest form as

$$P(\lambda, R) = K(\lambda, R)G(R)\beta(\lambda, R)T(\lambda, R). \tag{2.1}$$

It can be seen that the received power $P(\lambda, R)$ includes four factors. Going into more detail for each factor, the first factor in equation (2.1) $K(\lambda, R)$ represents the system factor and can be written as

$$K(\lambda, R) = P_0(\lambda)\frac{c\tau}{2}A\eta \tag{2.2}$$

where $P_0(\lambda)$ is the average power of a single laser pulse and τ [s] is the optical pulse width and $c\tau$ is the length of the laser pulse at a fixed time. The factor $1/2$ appears because the laser pulse has to travel forward and backward. A is the area of the primary receiver optics responsible for collection of backscattered light, and η is the overall system efficiency. It includes the optical efficiency of all elements such as the transmitter, receiver and the detection efficiency. It can be optimized for the best possible signal. The telescope area A $[m^2]$ and the average laser power $P_{avg}[W] = P_p{*}\tau/T$ (with P_p is peak power, τ is pulse width and T is the period of time, in inverse to the pulse repetition rate frequency f_{rep} [Hz]) are primary design parameters of a $LIDAR$ system.

The second factor in equation (2.1) $G(R)$ is a geometric factor, the ratio of the laser beam receiver-field-of-view overlap and the term R^2 and written as

$$G(R) = \frac{O(R)}{R^2} \tag{2.3}$$

The laser beam receive-field-of-view is the receiver telescope area or the entrance area of the telescope receiver. The quadratic reduction of the signal intensity with the distance (R[m]) is due to the fact that the receiver telescope area makes up a part of a sphere's surface with radius R that encloses the scattering volume. This leads to a strong influence on the received intensity. For example, a detected signal at 10 m with $O(R) = O(10) = 1$ will be 6 orders of magnitude lower at 10 km.

Both the first and second factors in equation 2.1 are completely determined by $LIDAR$ setup.

The third factor in equation (2.1) $\beta(\lambda, R)$ is the backscatter coefficient at the distance R. It is the subject of investigation, the primary atmospheric parameter that determines the strength of the $LIDAR$ signal and ascertains how much light is scattered into the backward direction, i.e towards the $LIDAR$ receiver. The backscatter coefficient is a specific value for the scattering angle of $\theta = 180^0$. If N_j is the concentration of scattering particles of kind j in the length of the laser duration pulse and the particles' differential scattering cross section for the backward direction at the wavelength λ is $\frac{d\sigma_{j,sca}(\pi,\lambda)}{d\Omega}$. The backscatter coefficient can be written as a sum of all kinds of scatters,

$$\beta(\lambda, R) = \sum\nolimits_j N_j(R) \frac{d\sigma_{j,sca}(\pi, \lambda)}{d\Omega}. \tag{2.4}$$

N_j is given in units of $[m^{-3}]$ and differential scattering cross section $(\frac{d\sigma_{j,sca}(\pi,\lambda)}{d\Omega})$ in $[m^2 sr^{-1}]$, the backscatter coefficient $(\beta(\lambda, R))$ has the unit $[m^{-1}sr^{-1}]$.

In the atmosphere, the laser light is scattered by air molecules and aerosols. It can be expressed as $\beta(\lambda, R) = \beta_m(\lambda, R) + \beta_a(\lambda, R)$ where β_m and β_a are the molecular and aerosol backscatter coefficients, respectively.

The final factor in equation (2.1) $T(\lambda, R)$ is the transmission term. It describes how much light gets lost on the way from the laser transmitter to the distance R and back. It is the subject for studying. It results from the specific form of the Lambert-Beer's law for $LIDAR$. Thus it can be values between 0 to 1 and given by

$$T(\lambda, R) = \exp\{-2 \int_0^R \alpha(\lambda, r)\mathrm{d}r\}. \tag{2.5}$$

The integral considers the path from the $LIDAR$ to the distance R. The factor 2 is due to two-way transmission path. The $\alpha(\lambda, r)[m^{-1}]$ is the extinction coefficient and is the product of number concentration $N_j(r)[m^3]$ and extinction cross section $\sigma_{j,ext}$ for each type of scatter j,

$$\alpha(\lambda, r) = \sum_j N_j(r)\sigma_{j,ext}(\lambda) \tag{2.6}$$

extinction is caused by both scattering and absorption of light and both by molecules and particles. The total extinction coefficient $\sigma_t(\lambda, r)[m^{-1}]$ thus includes molecular scattering and aerosol scattering, molecular and aerosols absorption. It can be expressed as

$$\alpha_t(\lambda, r) = \alpha_{m,sca}(\lambda, r) + \alpha_{a,sca}(\lambda, r) + \alpha_{m,abs}(\lambda, r) + \sigma_{a,abs}(\lambda, r) \tag{2.7}$$

The subscripts m and a stand for molecular and aerosol, sca and abs for scattering and absorption respectively. Due to scattering into all directions, the general extinction cross section is caused by the scattering cross section σ_{sca}, $[m^2]$ and the absorption cross section σ_{abs}, $[m^2]$. It can be written as

$$\sigma_{ext}(\lambda) = \sigma_{sca}(\lambda) + \sigma_{abs}(\lambda). \tag{2.8}$$

Finally, summarizing all the individual terms, the $LIDAR$ equation can be rewritten as

$$P(\lambda, R) = P_0 A\eta(\lambda)(\frac{c\tau}{2})\{\frac{O(R)}{R^2}\}\beta(\lambda, R)\exp\{-2 \int_0^R \alpha(\lambda, r)\mathrm{d}r\}. \tag{2.9}$$

Equation 2.9 is a common equation form of the $LIDAR$ system. Depending on interaction processes of the laser transmitter with the atmospheric constituents, $LIDAR$ systems can be classified into five different systems based on the specifically physical phenomenons such as elastic-backscatter, differential absorption, Raman, resonance fluorescence and

Doppler. The $LIDAR$ equation of each kind of $LIDAR$ therefore is also developed based on each physical interaction.

In this work, diode laser based $MOPA$ concepts suitable for elastic-backscatter and differential $LIDAR$ systems for aerosols and water vapor detection are demonstrated. In the following, a further discussion about these systems is given.

Elastic-backscatter $LIDAR$ is developed based on elastic scattering in which the wavelength is conserved with incident wavelength but its direction is modified. It provides information of the presence and location of aerosols and cloud layers. The system uses one laser emitting a single wavelength and one detector measuring the radiation elastically backscattered from the atmospheric molecules and particles. Depending on the size of the particles, elastic backscatting $LIDAR$ can be a *Rayleigh* or a *Mie LIDAR*. *Rayleigh* scattering can be defined as the elastic scattering from particles that are very small compared to the wavelength of the radiation (laser transmitter). Its scattering intensity is proportional to λ^{-4}.

In case of particles with sizes comparable to the wavelength of the radiation or larger, Mie scattering dominates. It is not limited to a certain size of the scatters. The scattered intensity is a function of particle radius relative to wavelength and the particles complex refractive index. Scattering from very large particles does not depend on the wavelength.

Because of the different shapes of particles in the atmosphere, Mie scattering theory is applied for providing a very rough approximation. Since the particles are small compared to the wavelength, the actual shape does not play a major role for the scattering properties as theories for not-spherical scatters show [35].

In general, both Rayleigh-Mie $LIDARs$ measure the total atmosphere backscatter without separation of particle and molecular contribution. They provide a rough profile of the climate relevant volume extinction coefficient of the particles.

The requirement of light source for these systems therefore is effortless to the spectral line width. The intensity of the backscattered signal is of interest, so that a laser with a broad spectral line width can be used. However, to suppress the sunlight background of the daytime operation,

Table 2.1.1: Parameters of light sources for elastic-backscatter *LIDAR* system for aerosols detection

Peak power: P_p	> 10 W
Pulse width: τ	< 10 ns
Repetition rate: f	> 20 kHz
Spectral linewidth: $\Delta\lambda$	< 300 pm
Wavelength: λ	1064 nm
ASE:	$< 10\%$

a filter of 300 pm is often used. Thus, a spectral line width of about 300 pm should be sufficient. The light sources with a high peak power to achieve a large signal-to-noise ratio are to be expected. In this work, a peak power of above 10 W with a repetition rate more than 20 kHz to achieve more photons backscatted to receiver are applied. A short pulse width provides a high resolution of the system. A single wavelength with certain wavelength to avoid uncertain in the laser line position which causes errors in measurement. A small amount of amplified spontaneous emission (ASE) provides a spectral purity which needs to prevent errors in measurement. These parameters are given in the table 2.1.1.

In order to provide accuracy and high resolution, e.g, water vapor profiling, the differential absorption $LIDAR$ or $DIAL$ is introduced.

2.2 Differential absorption LIDAR (DIAL) for gas measurements, e.g., water vapor profiling

Differential absorption $LIDAR$ ($DIAL$) technique uses two different wavelengths, one of which is absorbed more strongly than the other. The differential molecular absorption coefficient $\Delta\alpha_{mol,abs}$ can be determined, if the differential absorption cross section $\Delta\sigma_{mol,abs}$ for the two wavelengths is known. The number concentration of the gas atoms or molecules can be determined.

When two wavelengths are very close to each other in the spectral regions where any absorption by gases in the atmosphere is negligible except for water vapor absorption. Going into the elastic back scatter $LIDAR$ equation 2.9 as mention above, the factors such as system (K), geometric (G), backscatter coefficient (β) are equivalent for two wavelengths. Only the transmission term (T) factor is effected by wavelengths which is caused only by water vapor and induced by the Lambert-Beer's law. In the idealized case, the $LIDAR$ signal back scattering intensities are described as

$$P(\lambda, R) = P_0 A\eta(\frac{c\tau}{2})\{\frac{O(R)}{R^2}\}\beta(R)\exp\{-2\int_0^r \alpha(\lambda, r)\mathrm{d}r\}. \quad (2.10)$$

Therefore, the received power $P(\lambda, r)$ from range r at the wavelength (λ) is dependent on the wavelength, only by water vapor.

Applying for two wavelengths λ_{on} and λ_{off}, corresponding to larger and smaller absorption cross sections, then it is divided between each other and can be written

$$\frac{P(\lambda_{on}, r)}{P(\lambda_{off}, r)} = \frac{\exp\{-2\int_0^r \alpha(\lambda_{on}, r)\mathrm{d}r\}}{\exp\{-2\int_0^r \alpha(\lambda_{off}, r)\mathrm{d}r\}} \quad (2.11)$$

In the simplest form, it is set as:

$$P(\lambda_{on}, r) = P_{on}(r),\ P(\lambda_{off}, r) = P_{off}(r),$$
$$\alpha(\lambda_{on}, r) = \alpha_{on}(r),\ \alpha(\lambda_{off}, r) = \alpha_{off}(r) \quad (2.12)$$

The water vapor extinction coefficient is product of water vapor number density N_{WV} and the absorption cross section σ_{WV}. It is written as

$$\alpha_{WV} = \sigma_{WV}\ N_{WV} \quad (2.13)$$

And it can be set,

$$\alpha_{on} = \sigma_{on}\ N_{WV},\ \alpha_{off} = \sigma_{off}\ N_{WV} \quad (2.14)$$

Replaying the equations (2.12- 2.14) into the equation 2.11 and differentiating both sides of the equation, they can be written as

$$\ln\{\frac{P_{on}(r)}{P_{off}(r)}\} = \frac{\{-2\int_0^r \sigma_{on}\ N_{WV}\mathrm{d}r\}}{\{-2\int_0^r \sigma_{on}\ N_{WV}\mathrm{d}r\}} \quad (2.15)$$

The differential between the two spectral separated $LIDAR$ returns over an adjacent range, $dr = c\tau/2$, can be written as

$$\{\ln(P_{on}, r) - \ln(P_{on}, r + dr)\} - \{\ln(P_{off}, r)) - \ln(P_{off}, r + dr)\} = 2\int_{r}^{r+dr} \sigma_{on}\ N_{WV}\mathrm{d}r' - 2\int_{r}^{r+dr} \sigma_{off}\ N_{WV}\mathrm{d}r' \tag{2.16}$$

The molecular concentration in the Lambert-Beer's law relationship is also assumed to be a constant over a singe range dr, allowing the integral in equation 2.16 to be simplified as

$$\begin{aligned} 2\int_{r}^{r+dr} \sigma_{on}\ N_{WV}\mathrm{d}r' &= 2\sigma_{on}\ N_{WV}(r + \mathrm{d}r)\ dr \\ 2\int_{r}^{r+dr} \sigma_{off}\ N_{WV}\mathrm{d}r' &= 2\sigma_{off}\ N_{WV}(r + \mathrm{d}r)\ dr \end{aligned} \tag{2.17}$$

After algebraic manipulation the water vapor concentration can be written

$$N_{WV}(r + dr) = \frac{1}{2\ \sigma_{eff}(r)\ dr} \ln\{\frac{P_{on}(r)}{P_{on}(r + dr)} \frac{P_{off}(r + dr)}{P_{off}(r)}\} \tag{2.18}$$

where $\sigma_{eff}(r) = \sigma_{on}(r) - \sigma_{off}(r)$ is the effective cross section. The $dr = c\tau/2$ is the range size, $P_{on}(r)$, $P_{on}(r+dr)$, $P_{off}(r)$ and $P_{off}(r+dr)$ are the intensities coming back to receiver at the wavelengths online and offline at the range of r and $r + dr$, respectively. More details can be read in [35–37].

In practice, the $DIAL$ equation 2.18 is used to calculate the water vapor concentration. It is realized by forming the ratio with the above assumptions. Taken into account to achieve a accuracy measurement, the errors caused by detectors, atmospheric effects and laser transmitters should be minimized.

For detectors as background signal noise from solar radiation, the detector dark current and amplifier noise should be considered [38].

For atmospheric effects and laser transmitters, the main atmospheric effects include temperature sensitivities, pressure broadening and pressure shifts of the H_2O absorption lines, and Doppler broadening of the Rayleigh backscattered component in the $LIDAR$ return [36–42].

Table 2.2.1: Parameters of light sources for $DIAL$ for water vapor concentration detection in the lower troposphere in this work

Peak power: P_p	> 10 W
Pulse width: τ	8 ns
Repetition rate: f	25 kHz
Spectral linewidth: $\Delta\lambda$	< 10 pm
Wavelength: λ	975 nm, tunable
Wavelength: λ	965 nm, dual
ASE:	$< 1\%$

Thus laser transmitters for water vapor concentration should be chosen an appropriate absorption line strength for minimizing the absorption cross-section sensitivity to temperature, pressure broadening, etc, as well as isolated from other nearby absorption lines. The line width of light source smaller than spectral line width of the absorption line is requested. The spectral purity and a certain wavelength are also needed to limit the error in measurement.

Success in MPL system development is strongly connected with optical and electronic technology, in particular laser technology [35]. To meet the requirements of a certain MPL system, specifically designed lasers for laser power, pulse width, repetition rate, wavelengths, spectral line width and spectral purity are needed.

In this target, the main parameters of the laser systems are shown in table 2.2.1. A peak power more than 10 W with a high repetition rate provides a high photons backscatted to receiver. A spectral linewidth is smaller than the absorption line of the water vapor at the 975 nm region at the normal atmosphere. A short pulse width (8 ns) provides a high resolution of the system (1.2 m). A tunable wavelength to scan over several absorption lines of the water vapor for concentration calibration and selection the working points or a dual wavelength to switch on and off absorption line can be expected. A small amount of amplified spontaneous emission provides a spectral purity which needs to prevent errors in measurement.

More details of these parameters of light sources in the $MPLs$ systems, an analysis of each parameter is given in the following section.

2.3 Specific requirements of laser systems for LIDAR and DIAL

Going into detail of the contribution of each parameter of the light source of the $MPLs$ the specific parameters of diode laser based $MOPA$ systems in this work are clarified as following.

The first parameter is the peak power. A high value is desired for many applications. A peak power higher than 10 W is the target. For high energy of light sources is needed for $LIDAR$ systems, one can be used by high peak powers and low repetition rates and another can be applied by low peak powers with high repetition rates. In the case of repetition rates of 10 kHz, peak powers in the range between 2 W and 10 W with a pulse width of 1 μs were performed [22–26]. The water vapor profiling in the range of 7 km and a resolution of 150 m were reported in the measured time of about 10 minutes. Comparable with our systems, a peak power of more than 10 W at higher repetition rates (25 kHz) at the pulse width of 8 ns should be sufficient to provide a high backscattering signal. A shorter pulse width should provide a higher spatial resolution of the $LIDAR$ systems, and a higher repetition rate can be reduced the measurement time.

The second and third parameters are the pulse width and the repetition rate. The pulse width of the light sources determines the achievable spatial resolution in such systems whereas the repetition rate determines the possible measured range of the system [12, 28, 29, 43]. The explicit dependence of the resolution (ΔL) and measured range (L) on the pulse width and repetition rate of laser pulses, an example of two consecutive laser pulses is sketched in Fig. 2.2. The relevant return signals as well as the resolved-time interval are detected in the receiver. They are expressed on the time scale axis (t) and the distance scale axis (L) respectively. The symbols used to express the parameters are as follow: the pulse width (τ), the repetition rate (f), the measured range (L) and the resolution (ΔL).

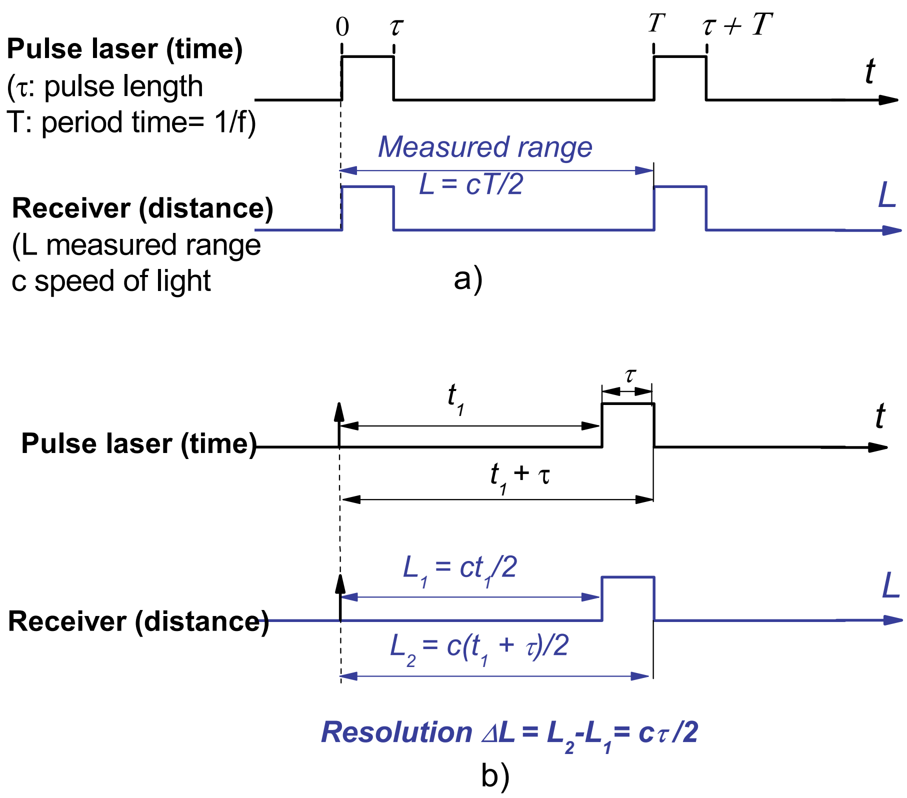

Figure 2.2: Schematic diagram of two consecutive laser pulses and relevant receiver for calculation the distance (a) and resolution (b) of the LIDAR system .

The measured range L is determined by comparing the time elapsed between the transmitted laser pulse and the return pulse T (corresponding to a repetition rate $f = 1/T$). It is calculated by $L = cT/2$. It is a product of the speed of the light (c) and the factor $1/2$ as the light has to travel forward and backward. A repetition rate between 1 MHz and 25 kHz, corresponding to the periods of time of 1 μs and 40 μs, is needed for a measured range between 330 m and 6000 m, respectively.

The resolution is estimated by the analog recording of the backscattered light. It depends on the pulse width τ according to $\Delta L = c\tau/2$ with c speed of light. At a certain measurement time t_1 signals from the leading edge of the pulse arrive at the detector from the position $L_1 = 1/2ct_1$ and from training edge is $L_2 = 1/2c(t_1 + \tau)$. The resolution (the difference of leading and training edge positions) is determined by $\Delta L = L_2 - L_1 = c\tau/2$. Thus, in order to obtain a resolution in the range from 0.3 m to 1.2 m, pulse widths between 2 ns and 8 ns are needed.